D. Shiozawa et alii, Frattura ed Integrità Strutturale, 33 (2015) 56-60; DOI: 10.3221/IGF-ESIS.33.07

3D Analyses of crack propagation in torsion

D. Shiozawa
Kobe University, 1-1, Rokkodai, Nada-ku, Kobe, Japan
shiozawa@mech.kobe-u.ac.jp

I. Serrano-Munoz, S. Dancette, C. Verdu, J. Lachambre, J.-Y. Buffiere
INSA-Lyon MATEIS Bat Saint Exupery 25 Av. Jean Capelle F-69621 Villeurbanne Cedex
jean-yves.buffiere@insa-lyon.fr

ABSTRACT. The initiation and propagation of fatigue cracks during cyclic torsion loading was studied in a cast Al alloy (A357) with a relatively large (~500 μm) grain size. 2D observations, revealed that multi site crack initiation occur on the {111} slip planes exhibiting the highest slip activity (iso-strain Taylor analysis), preferentially on planes nearly perpendicular to the sample axis. Within the first grain, the cracks have a pronounced crystallographic propagation mode (mode II crack growth) and strongly interact with the grain boundaries. In situ 3D monitoring of torsion fatigue tests using synchrotron X-ray tomography reveal that propagation towards the interior of the samples occurs first along the sample periphery in mode II leading to relatively shallow cracks which penetrate towards the sample center only after a large number of cycles is reached .The values of mode I, II and III stress intensity factors have been calculated from finite element simulation at the tip of the shallow mode II crack. Those values are used to analyse the bulk propagation of the observed cracks.

KEYWORDS. Torsion; Cracks; 3D imaging; Stress Intensity Factors; Mode III mode II.

INTRODUCTION

Since most machine components are operated under complex cyclic stress states, it is important to understand the propagation behavior of fatigue cracks under mixed loading. One of the most typical mixed mode crack propagation behavior arises under cyclic torsion. Compared to tensile uni-axial loading, in torsion, the planes of the specimen showing the largest of shear stresses values are not submitted to any normal stress. Besides, the level of the shear stresses is maximum at the sample surface and decreases towards the bulk of the sample. Those two distinctive features have a strong influence on the initiation and propagation of fatigue cracks.
Experimentally, in metals, fatigue crack propagation mechanisms in torsion have been mainly studied through surface observations [1, 2] or by *post mortem* fractographic analyses [3]. The link between surface observations and fracture surfaces where crack growth can be very complex is however difficult to establish and the detailed chronology of crack growth in the sample interior is lost. The 3D shape of a fatigue crack growing inside a Ti alloy has been analyzed using X ray tomography [4]; although this is a considerable improvement compared to the aforementioned observations the images were obtained during *ex situ* experiments providing pictures of unloaded cracks. In this paper, we report results on the initiation and propagation of fatigue cracks during cyclic torsion loading of a cast Al alloy (A 357). In situ experiments have been performed on macroscopic samples (surface monitoring by optical microscopy) and on smaller ones (bulk

characterisation by synchrotron X-ray tomography), providing a chronology of crack development with this loading mode both at the surface and in the bulk of the material. The observed crack paths are analysed in light of the mode I, II and II stress intensity factors obtained from finite element simulations.

EXPERIMENTAL SET UP

The material used in this study is a cast Aluminium alloy A357. The fatigue samples were cut from the central part of cylindrical rods (30 mm diameter) obtained by permanent mold casting. After a T6 treatment (solution treatment at 540°C for 10h followed by water quench and 8h at 160°C) the average Secondary Dendrite Arm Spacing (SDAS) was found equal to 38 µm and the average grain size to 501 µm; the value of the 0.2% yield stress obtained from tensile tests was 275 MPa. Macroscopic Torsion fatigue specimens were machined according to ISO-1352-2011 Standard [5] and reversed torque-controlled fatigue tests were carried out using a MTS 809 Axial/Torsional servohydraulic machine at a frequency of 10 Hz. A polished flat surface was produced along the cylindrical sample gage length in order to monitor crack development by in situ optical microscopy. Electron Back Scattered Diffraction observations of this surface were performed *post mortem*.

In situ reversed torque controlled torsion tests were also carried out at the European Synchrotron Radiation Facility (ESRF) on beamline ID19 on smaller samples (3mm diameter) in order to monitor crack initiation and growth in the bulk using X-ray tomography. The samples were cycled in situ with a dedicated rig and observed under load at the two extreme values of torque (+ τ_{max} and – τ_{max}). The sample shown here had been submitted to 195 kcycles at $|\tau_{max}|$=120 MPa before a first imaging scan was performed. Then a scan was recorded every 10 or 20 kcycles until 305 kcycles.

EXPERIMENTAL RESULTS AND DISCUSSION

On the first scan at 195 000 cycles at τ_a=120 MPa, vertical cracks (*ie* cracks which intersection with the sample surface is aligned with the cylindrical sample axis) and horizontal cracks (*ie* crack perpendicular or nearly perpendicular to the sample axis) were observed. An optical image of one horizontal crack is shown on Fig. 1.

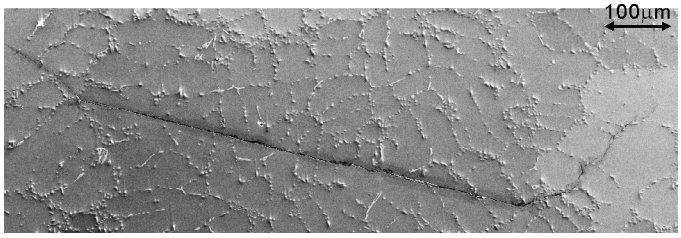

Figure 1: Optical micrograph of a mode II intragranular crack fatigue crack observed after 100 000 kcycle (τ_{max}=95 MPa). The sample axis is vertical on the figure. The plane of the crack correspond to a {111} plane the white lines show the grain boundaries with two neighbouring grains.

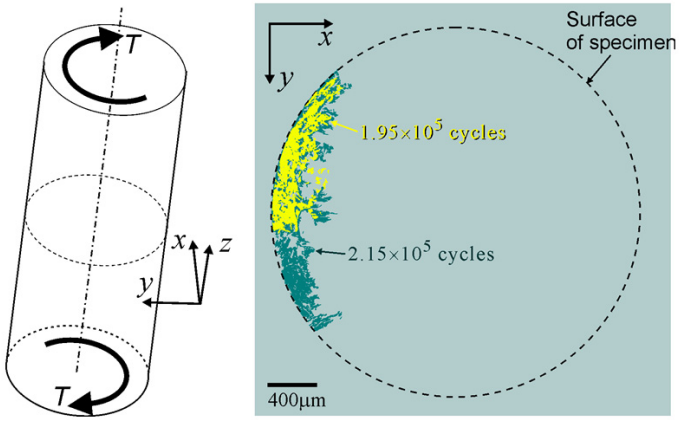

Figure 2: 3D rendering of a crack perpendicular to the sample axis similar to the one shown in Fig. 1 at two different numbers of cycles.(195k cycles and 215k cycles).

EBSD analysis has revealed that such cracks form on the {111} planes which experience the highest slip activity (iso strain Taylor analysis) [5]. A strong interaction with the grain boundaries is observed, generally accompanied by a pronounced change of direction. The sub-surface development of such a crack can be observed at 195,000 and 215,000 cycles in Fig. 2. From the various images recorded in 3D, we observed that Mode II growth (at the intersection of the crack tip with the surface) was faster than mode III growth (in the bulk). This is shown in Fig. 3 where one can observe that the crack length on the surface c increases rapidly with increasing in number of cycles N and tends to saturate when a crack length of the order of 3mm is reached. The sub surface crack length a increases almost linearly, and less rapidly, as a function of N. The crack arrest and/or decrease in crack propagation rate in Mode II crack has been linked in the literature to crack tip shielding [6, 7] induced by the friction between the crack surfaces (some debris between the crack surfaces have been observed in the interior of the sample as well as at the surface).

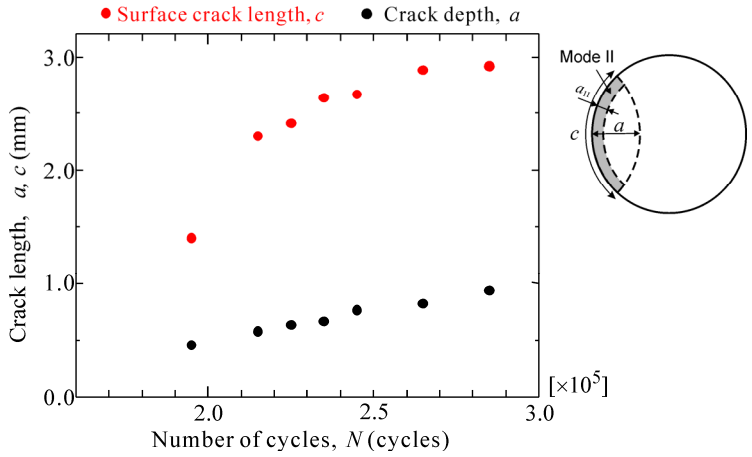

Figure 3: Crack growth curve of the crack shown in Fig. 2: surface growth (mode II) is more rapid than bulk growth.

After a rapid intragranular propagation below the surface in mode II, cracks similar to those shown in Fig. 1 and 2 will eventually grow toward the interior of the sample. This second stage of propagation corresponds however to a change in mode as can be seen on Fig. 4. Fig. 4(c) show reconstructed images parallel to the z-axis, and at various depth within the bulk as indicated by the white lines shown in Fig. 4(a). One can clearly see that when moving from the surface towards the interior the cracks evolve from a (nearly) horizontal orientation towards a 45° orientation (with respect to the z-axis) corresponding to a gradual change from mode III towards mode I opening.

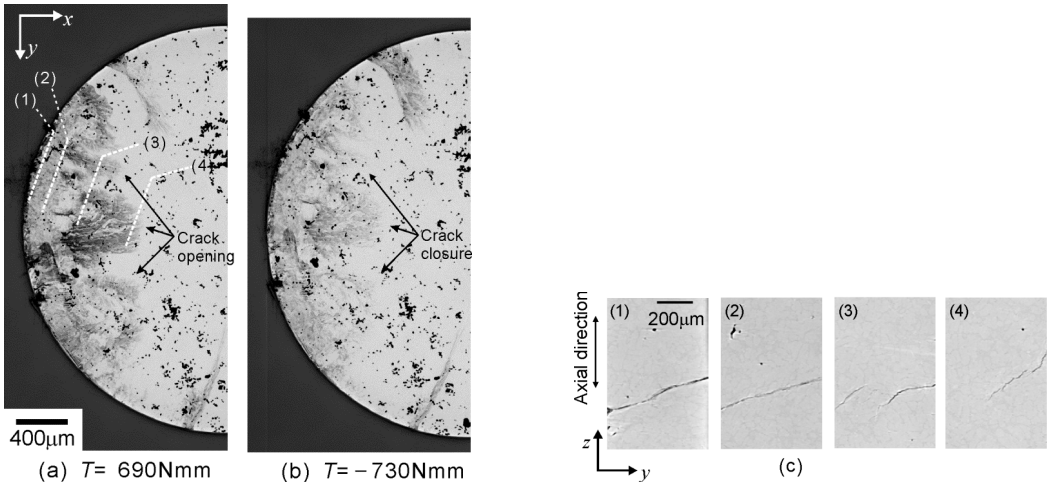

Figure 4: (a) and (b): projection along the z axis of the minimum intensity in the reconstructed volume of the sample after 265k cycles, (c) vertical slice at the positions indicated by the white lines.

Fig. 4(a) shows a projection of the minimum intensity of the voxels of the reconstructed volume of the sample along the z direction. A crack (or a porosity) which shows little attenuation appears in black on such projections and a darker grey

level corresponds to a larger opening of the crack (or to a larger porosity) and vice versa. With this type of rendering, the closing/opening of some parts of the crack open in mode I below the surface under the application of the positive or negative torque can clearly be observed. To discuss the change of crack propagation mode from Mode III to Mode I in the bulk of the sample, the values of stress intensity factors for a crack in torsion have been calculated by FEM analysis. The FEM model used is shown in Fig. 5: a crack of depth a_{II} (a_{II} =180μm) similar to the crack shown in Fig. 2 is modeled. The distribution of the stress intensity factor values along the crack tip for a circumferential length c=0.25mm is shown in Fig. 6. As expected, K_I is equal to 0 all along the crack front. On the contrary, K_{II} is maximum at the point corresponding to the intersection between the crack tip and the surface and is equal to 0 inside the sample. K_{III} is maximum inside the sample. Several calculations have been performed with increasing values of c. It is found that when c increases, K_I remains equal to 0 and, after a slight increase, the K_{II} values saturate . Although the change in crack propagation mode inside the sample cannot be correlated to the calculated distribution of K_I, the saturation in crack growth rate observed for intragranular growth could be the result of the saturation observed for K_{II} values when c increases.The stress intensity values found from our model cannot therefore account for the transition between mode III to mode I observed in the bulk. However, it can clearly be observed from Fig. 1 that when meeting a grain boundary the observed fatigue cracks can be strongly deflected. This could also happen in the bulk. If a small kink crack forms at the crack tip in the bulk (or at the surface), because of the local crystallography, the values of the mode I stress intensity factor will increase rapidly [4] and mode I growth can take place.

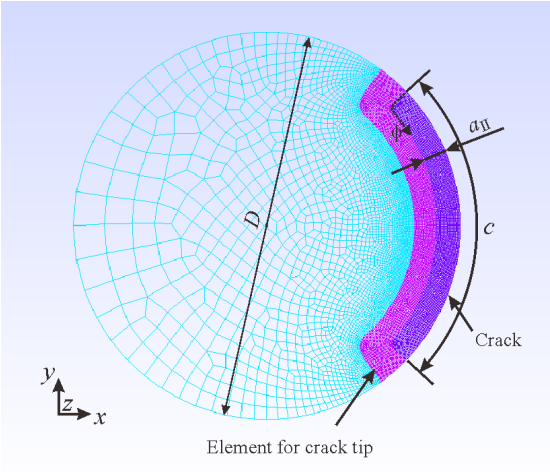

Figure 5: FEM model (a_{II}=0.18mm, D=3.5mm).

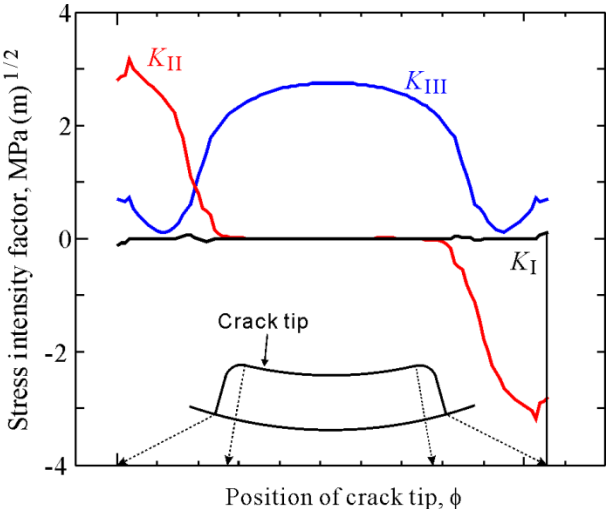

Figure 6: Stress intensity factor of stress intensity factor along crack front for a circumferential length c=0.25mm, τ=120MPa.

CONCLUSIONS

The mechanisms of crack initiation and propagation during cyclic reversed torque controlled experiment have been studied in situ. Surface observations (optical microscopy and EBSD) show that intragranular cracks initiate in mode II and have a strong cristallographic character. The planes of these cracks correspond to highly activated {111} slip planes. Strong deviations are often observed when those mode II cracks encounter some grain boundaries. The bulk development of those cracks has been imaged inside the sample bulk by synchrotron X-ray tomography. The crack growth rate at the surface (mode II) is faster than in the bulk (mode III) leading to a shallow crack. Friction between the crack surfaces might impede mode III growth in the bulk for low values of the applied torque. When the number of cycles is increased, however, the growth in the bulk resumes but in mode I. The values of the mode I, II and III stress intensity factors computed from a FE simulation cannot account for this transition from mode III to mode I unless some kink appears at the crack tip. Such a kink might be produced by a change in the local crystallography (grain boundary) as observed for the mode II cracks at the surface.

REFERENCES

[1] Murakami Y, Takahashi K, Toyama K., Mechanism of crack path morphology and branching from small fatigue cracks under mixed loading. Fatigue Fract Engng Mat Struct, 28(1–2) (2005) 49–60.
[2] Sawada M, Bannai K, Sakane M., Crack propagation of type 304 stainless steel in torsion low cycle fatigue, J Soc Mat Sci Jpn, 54(6) (2005) 615–21.
[3] Murakami, Y., Takahashi, K., Kusumoto, R., Threshold and growth mechanism of fatigue cracks under mode II and III loading, Fatigue Fract Engng Mater Struct 26(2003), 523–531.
[4] Shiozawa, D., Nakai, Y., Murakami, T., Nosho, H., Observation of 3D shape and propagation mode transition of fatigue cracks in Ti–6Al–4V under cyclic torsion using CT imaging with ultra-bright synchrotron radiation, Int. J. Fatigue, 58 (2013) 158-165.
[5] PhD I.Serrano Munoz INSA Lyon (2014), http://theses.insa-lyon.fr/publication/2014ISAL0117/these.pdf (in english)
[6] Matsunaga, H., Muramoto, S., Shomura, N., Endo, M., Shear mode growth and threshold of small fatigue cracks in SUJ2 bearing steel, J Soc Mat Sci Jpn, 58(9) (2009) 773–80.
[7] Campbell, JP, Ritchie, RO. Mixed-mode, high-cycle fatigue-crack growth thresholds in Ti–6Al–4V: II. Quantification of crack-tip shielding, Eng Fract, Mech, 67 (2000) 229–49.